3D Printing of Concrete with a Continuum Robot Hose Using Variable Curvature Kinematics

Manu Srivastava
Dept. Electrical and Computer Engineering
Clemson University
Clemson, USA
manus@g.clemson.edu

Jake Ammons
Dept. Electrical and Computer Engineering
Clemson University
Clemson, USA
jlammon@g.clemson.edu

Abdul B. Peerzada
Dept. Civil Engineering
Clemson University
Clemson, USA
apeerza@g.clemson.edu

Venkat N. Krovi
Dept. Automotive Engineering
Clemson University
Clemson, USA
vkrovi@clemson.edu

Prasad Rangaraju
Dept. Civil Engineering
Clemson University
Clemson, USA
prangar@clemson.edu

Ian D. Walker
Dept. Electrical and Computer Engineering
Clemson University
Clemson, USA
iwalker@g.clemson.edu

***Abstract*—We present a novel application of continuum robots acting as concrete hoses to support 3D printing of cementitious materials. An industrial cement hose was fitted with a cable harness and remotely actuated via tendons. The resulting continuum hose robot exhibited non constant curvature. In order to account for this, a new geometric approach to modeling variable curvature inverse kinematics using Euler curves is introduced herein. The new model does not impose any additional computational cost compared to the constant curvature model and results in a marked improvement in the observed performance. Experiments involving 3D printing with cementitious mortar using the continuum hose robot were also conducted.**

***Index Terms*—continuum, kinematics, variable curvature, concrete**

I. Introduction

This paper addresses challenges in deploying a continuum manipulator exhibiting non-constant curvature in a novel, large-scale application: that of 3D printing of concrete in construction operations. Continuum/soft robots are often inspired by nature, e.g., an elephant's trunk or an octopus' arm [22], and represent a paradigm change from rigid link robots capable of displacement at a finite number of joints to a compliant structure capable of bending at any point along its length. Their design allows them to access spaces that are unreachable using traditional robots or grasp objects by winding their body around them as opposed to using an end effector with force sensors at the end of a rigid link arm.

However, these capabilities come at the cost of lower weight bearing capacity and end effector positioning accuracy. In spite of these shortcomings, and in large part due to research advances in kinematics and dynamics of continuum sections, continuum robots have found uses in minimally invasive surgery [5], exploration [8], [17], toxic waste removal [13], and turbine inspection and repair [10].

This work is supported by the U.S. National Science Foundation under grants 1924721 and 1718075.

Assuming that the bending occurs in a curve with constant curvature results in the most widely used kinematic models describing the shape of a continuum section [1], [11], [15], [24], [23]. However, constant curvature models become inadequate when more accuracy is desired, precluding open loop control. The issue of non-constant curvature affects continuum sections when they operate against gravity or when underlying forces/torques, e.g. due to non-uniform mass distribution, and are not sufficiently modeled by the kinematics. Variable curvature is a particularly significant issue in the type of large-scale, high payload, high accuracy concrete printing application considered herein.

Construction with 3D printed structures has the potential to be cheaper, quicker, and ecologically friendlier than the traditional process by reducing the need for manual labor in the forming of blocks and transporting them to the construction site. Another major motivation for automated 3D concrete printing is that it allows building freeform structures without erecting complex and expensive formwork. In addition, reducing manual labor reduces the potential for workplace injuries and can result in long term cost savings [2].

There have been previous efforts aimed at 3D printing of concrete with traditional robotic systems. Various techniques investigated include gantry based systems [4], robotic arms on mobile bases [21] working collaboratively [20], and minibuilders - three small mobile robots to work on different aspects of concrete deposition [18].

We propose a novel alternative in which we adapt the concrete hose - an integral component of all the above approaches - to become a continuum robot. This is especially beneficial in space and weight constrained construction applications, e.g., extra-terrestrial applications and hard-to-reach places. This robotic hose could provide existing gantry based systems, cable driven parallel robots [7], and aerial platforms the ability to deposit concrete at a range of angles including

but not limited to vertically downwards.

This application requires greater accuracy than most continuum robot applications so far. However, the concrete hose presents non-constant curvature. The issue of modeling of variable curvature continuum sections has been addressed in prior works using a few approaches. One approach involves breaking the continuum section into several pieces assuming piecewise constant curvature. The work in [16] and [9] used such a model and used velocity Jacobian and particle swarm optimization based inverse kinematics respectively.

Mechanics based models, such as a model based on absolute nodal coordinate formulation developed in [14], are able to account for external loading. The authors of [6] used Cosserat beam theory to model a continuum section with multiple flexible backbones. A finite element method based approach was used in [3] but its complexity requires offline processing. The approach in [19] developed forward and inverse variable curvature kinematics based on Pythagorean hodographs.

All the above approaches need more computation than is feasible to perform in real-time in a construction environment. The authors in [12] introduced the idea of Euler curves to kinematically model a continuum section but traversed a middle ground by incorporating Euler curve based curvature variation in a constant curvature forward kinematics model. In this paper, we propose a new inverse kinematics model describing linearly increasing curvature based on Euler curves that imposes no additional computational cost compared to the constant curvature model, and is shown to be effective for the novel concrete printing application as demonstrated experimentally.

The paper is organized as follows. In section II, our method for the conversion of industrial concrete hoses to tendon-actuated continuum robots is introduced, and the construction of a two-section prototype described. A new approach for variable curvature inverse kinematics, needed to compensate for the non-constant curvature exhibited by the prototype, is introduced in section III. Implementation of the approach, and experiments with the prototype, are described and discussed in section IV. Section V concludes this manuscript.

II. 3D Printing of Concrete with Continuum Robot Hoses

A. Our Approach

The construction industry is a huge potential application area for robotics. Within the industry, the pouring of concrete is very important. The work presented herein forms part of a wider effort by the authors in the development of an innovative robotic system to interactively assist construction workers to dexterously deploy concrete-delivery hoses in congested spaces for 3D printing of concrete. The key component of that system is a novel cable-driven macro/micro design: a parallel cable-robot acts as macro-base, and a continuum robot (integrated with concrete delivery hose) acts as as micro-unit (Fig. 1). The goal is for the overall system to be rapidly field-deployable with a large workspace and high load carrying capability.

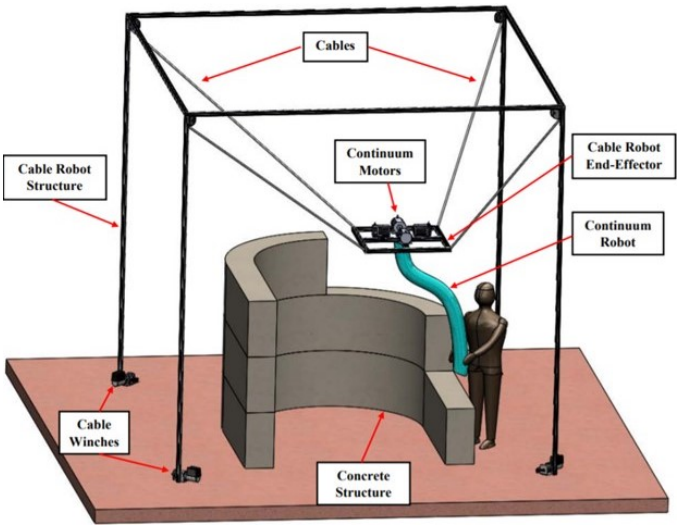

Fig. 1: Macro/micro robotic system for 3D concrete printing

In this paper, we describe the design and development of the micro-cable hose unit, realized as a tendon-actuated continuum robot. In this section, we describe the design and construction of a prototype cable hose. Its modeling and implementation are discussed in the following two sections.

B. Prototype

We designed and constructed a two section, six tendon driven continuum hose prototype with an industrial wire reinforced 2" ID shotcrete hose as its backbone due to its versatility in the construction industry. Since the backbone is not extensible, each section provides 2 Degrees of Freedom (DoFs), the plane of bending and the curvature in that plane. The resulting 4 DoFs provide 2 DoFs of kinematic redundancy when used to control 2 DoFs in the end effector/nozzle's orientation. (The third orientation DoF corresponds to torsion which is not achievable by the physical hose.) Such a system needs to be attached to an external platform with at-least 3 positional DoFs for the nozzle to have 5 DoFs in the task space. A limited few types of concrete structures could, however, be built with the continuum robot mounted to a platform restricted to vertical axis control, e.g. a cylinder and a wall. This work is limited to the description, kinematics, and control of the continuum robot mounted to a fixed external enclosure and associated experiments.

The driving assembly of the hose is attached to the external enclosure and acts upon the hose from above. Each section of the hose has length 0.7m and is actuated by three steel tendons separated by 120°, and the tendons are attached to the hose by five evenly spaced collars per section. The 3D printed collars are held on to the hose via hose clamps, and friction is reduced by routing the cables through offset bearings in the spacers (Fig. 2). The tendons for the distal section (containing the nozzle) pass through the proximal section's collars at an offset of 60° from its tendons.

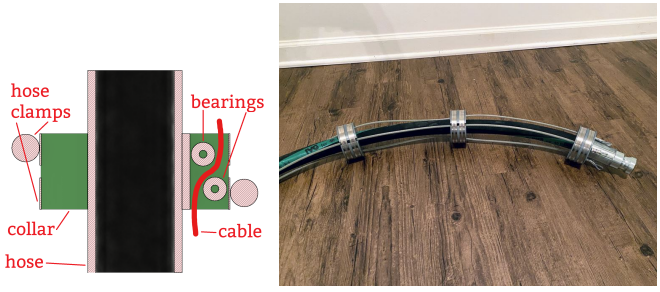

(a) Collar (b) Hose

Fig. 2: Hose assembly

Due to the weight of the hose imposing a high-power requirement, each tendon is actuated using a separate 110V AC-12V DC 40A power supply connected to a 25A MOSFET H-bridge motor driver, DC motor (5300RPM,133A stall current), and 100:1 drive reduction gearbox attached to a 3-D printed capstan on which the tendon is wound (Fig. 3). An Arduino microcontroller is used to implement position-control of tendon lengths calculated by a linear transform of the shaft angle sensed by absolute encoders.

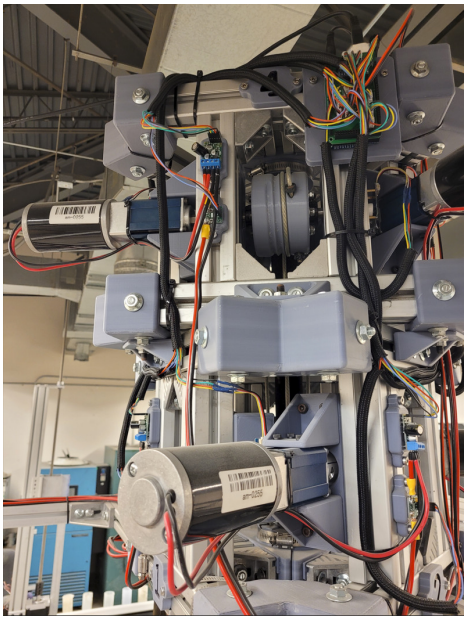

Fig. 3: Drive assembly

Initial experiments demonstrated that the robot does not exhibit constant curvature in either section. The key cause of this is gravity operating on the relatively heavy hose. Additionally, the distal section loads the end of the proximal section causing it to bend less than the constant curvature estimate. A similar effect is seen on the distal section due to a heavy metallic end that is standard on such hoses, resulting in uneven weight distribution across the length of the section. Therefore, variable curvature kinematics are required that can describe that the majority of the bending occurs near the end of the sections. We introduce such a model, based on Euler curves, in the next section.

III. KINEMATICS

In the past, Euler curves have been applied to continuum robot backbones as overlays in post processing [12], however inverse kinematics incorporating Euler curves, necessary for real-time control, had not been developed. This work provides a new approach to move from shape space (defined below as constant s, ϕ, and variable k) to the actuator space comprising of tendon lengths for two non-extensible sections using Euler curves.

A. Euler Curves

Given a smooth curve with curvature k defined by

$$k = d\theta/ds \tag{1}$$

where s is the curve length till the point at which k is being measured and θ is the angle between the initial tangent to the curve and the tangent at that point (Fig. 4), Euler curves are defined as those for which curvature increases linearly with the curve length s. One class of Euler curves, used herein,

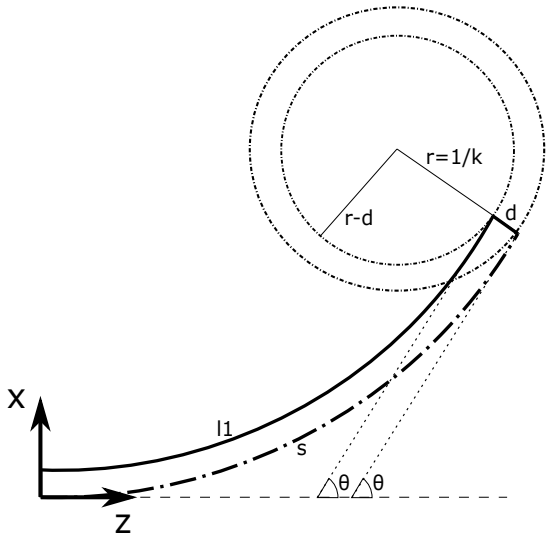

Fig. 4: Half section (split lengthwise) and Euler curves

parameterizes the curve by

$$k = 2a^2 s \tag{2}$$

with $2a^2$ is the constant of proportionality. Substituting (2) in (1) and integrating over the curve length,

$$\theta = 2a^2 \int_0^s u\, du = (as)^2 \tag{3}$$

B. Single Section Variable Curvature Inverse Kinematics

Equation (3) gives the orientation of every point on the Euler curve, θ, as a function of curve length, s. This curve is used to model the backbone of a constant length continuum section bending in the $\phi = 0$ rads plane - the plane containing tendon 1 by convention, and bending towards it. Tendon 1 is modeled by another Euler curve offset by half the section thickness, $(2d)/2$ (Fig. 4). The curvature of tendon 1, k_1, is given by,

$$k_1 = 1/(r - d) = d\theta/dl_1 \tag{4}$$

where l_1 is length of tendon 1 corresponding to the point with the same orientation, θ, as that at the point in the backbone where k is being measured. These points are located at a cross-section of a continuum section, assuming that planar cross-sections remain planar during bending. Following the same procedure as before,

$$k_1 = 2b^2 l_1 \tag{5}$$

$$\theta = (bl_1)^2 \tag{6}$$

where b is the constant of proportionality for tendon 1's Euler curve. Using (3) and (6),

$$bl_1 = as \tag{7}$$

and using (4) and (5),

$$b = \sqrt{1/(2l_1(r-d))} \tag{8}$$

and using (1) and (2),

$$r = 1/2a^2 s \tag{9}$$

Substituting (9) and (8) in (7) gives,

$$l_1 = s - 2(as)^2 d = s - 2\theta d \tag{10}$$

Equation (10) is valid throughout the backbone but is most useful when applied to the end point of the section using shape space parameters, s_{tip}, θ_{tip}, for a variable curvature section.

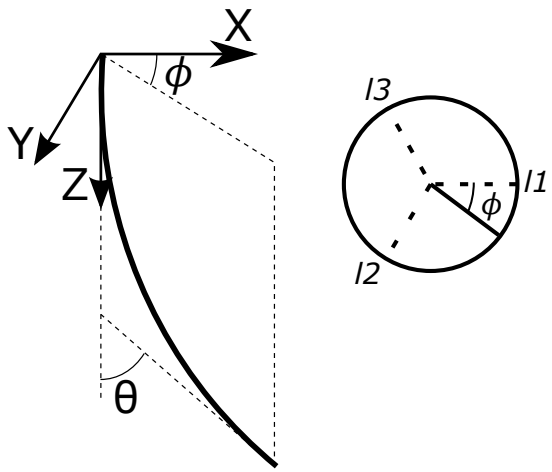

Fig. 5: Coordinate frame and tendon locations

Assuming that the tendon lengths can be projected onto an arbitrarily chosen plane of bending, ϕ (Fig. 5), [25], curvatures, k_1, k_2, k_3, at the projected locations are given by

$$k_1 = 1/(r - dcos(\phi)) \tag{11}$$

$$k_2 = 1/(r - dcos(2\pi/3 - \phi)) \tag{12}$$

$$k_3 = 1/(r - dcos(4\pi/3 - \phi)) \tag{13}$$

Following the same method as before yields the tendon lengths at the tip, $l_{1,tip}, l_{2,tip}, l_{3,tip}$,

$$l_{1,tip} = s_{tip} - 2\theta_{tip} dcos(\phi) \tag{14}$$

$$l_{2,tip} = s_{tip} - 2\theta_{tip} dcos(2\pi/3 - \phi) \tag{15}$$

$$l_{3,tip} = s_{tip} - 2\theta_{tip} dcos(4\pi/3 - \phi) \tag{16}$$

The above equations hold under the assumption that the tendons are curves or that the number of segments in a section tends to ∞. In reality, tendons are straight lines between the segments but the difference in lengths at the scale of the robot is not significant.

C. Two Section Variable Curvature Inverse Kinematics

Adding a second distal section in series with the first section needs three additional equations for its tendons which are at a 60° offset from the proximal tendons.The new tendon lengths, $l_{4,tip}, l_{5,tip}, l_{6,tip}$, where subscripts $_p$ and $_d$ denote proximal and distal properties at the end of the section, respectively, are given by,

$$l_4 = s_p - 2\theta_p dcos(\pi/3 - \phi_p) + s_d - 2\theta_d dcos(\pi/3 - \phi_d) \tag{17}$$

$$l_5 = s_p - 2\theta_p dcos(3\pi/3 - \phi_p) + s_d - 2\theta_d dcos(3\pi/3 - \phi_d) \tag{18}$$

$$l_6 = s_p - 2\theta_p dcos(5\pi/3 - \phi_p) + s_d - 2\theta_d dcos(5\pi/3 - \phi_d) \tag{19}$$

where the global distal bending plane angle, ϕ_d is given by

$$\phi_d = \phi_p + \phi_{d,local} \tag{20}$$

and $\phi_{d,local} = 0$ at the end-point of tendon 1 and is measured anticlockwise.

The above variable curvature inverse kinematics model was implemented on the two-section hose robot, with the results summarized in the following section.

IV. Implementation

In this section we describe validation and testing using the continuum hose robot prototype, as well as initial experiments in 3D printing of suitable cementitious materials.

A. Validation of Variable Curvature Kinematics

The kinematic model proved highly effective in compensating for the variable curvature exhibited by the robotic hose. We illustrate this via two sample experiments with the system.

Fig. 6 shows the distal section bent at $\theta = \pi/2$ in the $\phi = \pi/3$ bending plane containing tendon 4 using constant curvature kinematics (left) and Euler curve based variable kinematics (right). In a two-section experiment shown in Fig. 7, both, proximal and distal sections were actuated to $\theta_p = \pi/2$ and $\theta_d = \pi/2$ in the $\phi_p = 0$ and $\phi_d = \pi$ bending planes.

Both experiments depict a marked improvement in achieving the target orientation at the end of the section when using the Euler curve based kinematics. Note that constant curvature modeling, when implemented on the hardware, fails to calculate the necessary tendon lengths corresponding to the desired configuration. However, the variable curvature model introduced herein does generate the required tendon lengths.

It was noted empirically that higher initial tensions in the tendons when the hose is straight result in increased

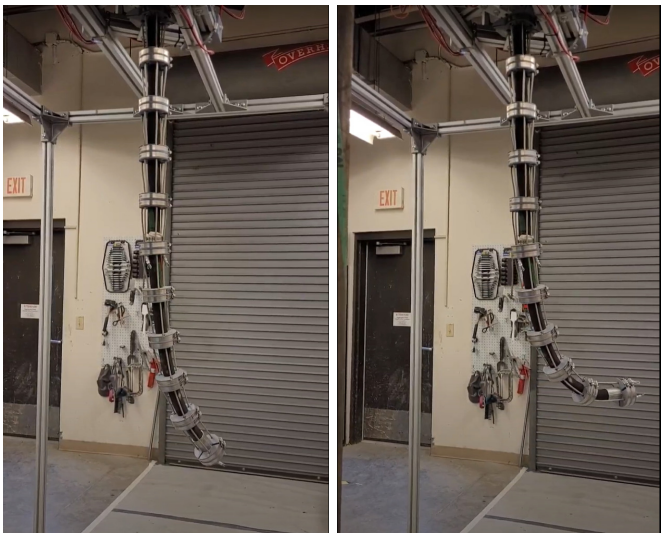

(a) Constant curvature (b) Variable curvature

Fig. 6: Distal bending

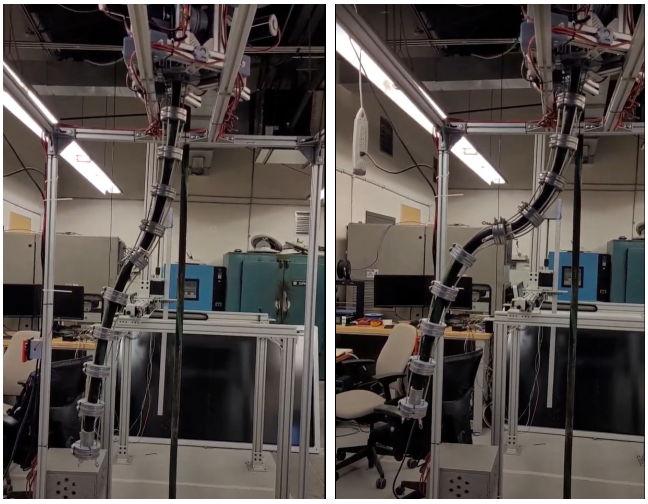

(a) Constant curvature (b) Variable curvature

Fig. 7: Bending in both sections

bending in both experiments. Since force/tension effects are unmodeled in kinematics, the tendons are manually pre-tensioned to empirically determined values at the start of the motions and not manually altered in between the kinematic comparisons.

B. Experiments in 3D Printing of Mortar

In a proof-of-concept demonstration of the functionality of the system, mortar was pumped through the robotic hose prototype. As a prerequisite for these experiments, fundamental research in cementitious materials suitable for 3D printing with the hose was conducted. A mortar mix with required rheological and stiffening requirements was developed. The mortar was based on a binder 80 percent by mass Type III cement and 20 percent by mass metakaolin, a water-to-cement binder of 0.38, sand-to-cement ratio of 1.2, a high range water reducer dosage of 5 mL/kg of binder and viscosity modifying agent at a dosage of 3 mL/kg of binder.

The mortar was pumped through a progressive cavity pump (MAI 2PUMP-PICTOR) with a flow rate range of 2-15 l/min and a maximum pressure capacity of 15 bars. The pump was equipped with a WIKA A10 pressure sensor and two pipe mounted vibrators to actively control the rheological properties of the mortar. However, in proof-of-concept studies the active control system was not used.

The platform height on which the mortar was deposited was controlled manually while the end-effector moved in a triangular trajectory. The trajectory was defined in the shape space - $\theta = \pi/2$ at $\phi = [0, 2\pi)$ since this was easier than defining the trajectory in the task space and the printed structure did not need to conform to a fixed set of Cartesian coordinates. The trajectory was broken down into numerous set-points using interpolation in the shape space and the constant time needed to reach each set-point (and hence the uniform end-effector speed) was determined empirically.

The key goal of the pumping of cementitious materials was to evaluate the effect of the movement of the hose/continuum robot on the pumping pressure of the progressive cavity pump. It was observed that the movement of the continuum hose does not significantly impact the inline pressure of the pumping setup. The system operated smoothly, and successfully printed multiple layers of mortar across the commanded profile (Fig. 8).

Fig. 8: Concrete printing with cable hose robot

V. Conclusions

One way in which automation and robotics are likely to disrupt the construction industry in the near future is via additive manufacturing. 3D printed structures are cheaper and more ecologically friendly than traditionally constructed ones. In addition, they are quicker to build and reduce workplace injuries.

Unlike other large scale 3D printing robots which use a passive hose for transporting a cementitious mixture to the printing nozzle, our approach removes additional bulk and weight by making the hose itself robotic, using a tendon driven cable harness. The resulting 2-section active continuum hose prototype is capable of dexterous manipulation. This is a new application of continuum robots and is challenging due to the inherent high accuracy requirements of 3D printing. Prior work with continuum robots has typically not required such high end effector placement accuracy relative to the scale of the robot.

During initial experiments, it was observed that gravity and unmodeled uneven mass distribution affected the curvature of both the sections and that constant curvature models could not be used to predict the nozzle orientation. A contribution of this work is the development of a geometric variable curvature inverse kinematic model based on Euler curves that is consistent with the observation that most of the bending occurs at the end of each section. Moreover, unlike other proposed variable curvature models, our new model does not impose additional computational cost compared to the constant curvature model. The nozzle orientation described by the new model was successfully verified experimentally. The active hose was used to 3D print a triangular structure using mortar in a proof of concept experiment.

REFERENCES

[1] T.F. Allen, L. Rupert, T.R. Duggan, G. Hein, and K. Albert, "Closed-Form Non-Singular Constant-Curvature Continuum Manipulator Kinematics", Proceedings IEEE International Conference on Soft Robotics (RoboSoft), Yale University, CT, (Online), pp. 410-416, 2020.

[2] J. J. Biernacki et al., "Cements in the 21st century: Challenges, perspectives, and opportunities," J. Am. Ceram. Soc., vol. 100, no. 7, pp. 2746–2773, 2017.

[3] T. M. Bieze, F. Largilliere, A. Kruszewski, Z. Zhang, R. Merzouki, and C. Duriez, "Finite Element Method-Based Kinematics and Closed-Loop Control of Soft, Continuum Manipulators," Soft Robotics, vol. 5, no. 3, pp. 348–364, Jun. 2018, doi: 10.1089/soro.2017.0079

[4] F. Bos, R. Wolfs, Z. Ahmed, and T. Salet, "Additive manufacturing of concrete in construction: potentials and challenges of 3D concrete printing," Virtual Phys. Prototyp., vol. 11, no. 3, pp. 209–225, 2016.

[5] J. Burgner-Kars, D.C. Rucker, and H. Choset, "Continuum Robots for Medical Applications: A Survey", IEEE Transactions on Robotics, Vol. 31, No. 6, December 2015, pp. 1261-1280.

[6] Y. Chen, B. Wu, J. Jin and K. Xu, "A Variable Curvature Model for Multi-Backbone Continuum Robots to Account for Inter-Segment Coupling and External Disturbance," IEEE Robotics and Automation Letters, vol. 6, no. 2, pp. 1590-1597, April 2021, doi: 10.1109/LRA.2021.3058925.

[7] P.C. Chesser, P.L. Wang, J.E. Vaughn, R.F. Lind, and B.K. Post, "Kinematics of a Cable-Driven Robotic Platform for Large-Scale Additive Manufacturing", ASME Journal of Mechanisms and Robotics, in press, 2021.

[8] M.M. Coad, L.H. Blumenschein, S. Cutler, J.A.R. Zepeda, N.D. Naclerio, H. El-Hussieny, U. Mehmood, J-H Ryu, E.W. Hawkes, and A.M. Okamura, "Vine Robots", IEEE Robotics and Automation Magazine, pp. 120-132, September 2020.

[9] S. Djeffal, A. Amouri, and C. Mahfoudi,"Kinematics Modeling and Simulation Analysis of Variable Curvature Kinematics Continuum Robots," in UPB Scientific Bulletin 2021, Series D: Mechanical Engineering. 83. 28-40.

[10] X. Dong, D. Axinte, D. Palmer, S. Cobos, M. Raffles, A. Rabani, and J. Kell, "Development of a Slender Robotic System for On-Wing Inspection/Repair of Gas Turbine Engines", Robotics and Computer-Integrated Manufacturing, April 2017.

[11] I.S. Godage, E. Guglielmino, D.T. Branson, G.A. Medrano-Cerda, and D.G. Caldwell, "Novel Modal Approach for Kinematics of Multisection Continuum Arms", Proceedings IEEE/RSJ International Conference on Intelligent Robots and Systems (IROS), San Francisco, CA, pp. 1093-1098, 2011.

[12] P. Gonthina, A.D. Kapadia, I.S. Godage, and I.D. Walker, "Modeling Variable Curvature Parallel Continuum Robots Using Euler Curves", Proc. IEEE International Conference on Robotics and Automation (ICRA)", Montreal, Canada, May 2019, pp. 1679-1685.

[13] R.E. Graham and R.E. Bostelman, "Development of the EMMA Manipulator for Hazardous Waste Remediation", Proceedings American Nuclear Society Seventh Topical Meeting on Robotics and Remote Systems, Augusta, GA, pp. 646-650, 1997.

[14] X. Huang, J. Zou and G. Gu, "Kinematic modeling and control of variable curvature soft continuum robots," IEEE/ASME Transactions on Mechatronics, doi: 10.1109/TMECH.2021.3055339.

[15] B. A. Jones and I. D. Walker, "Kinematics for Multisection Continuum Robots," IEEE Transactions on Robotics, vol. 22, no. 1, pp. 43–55, Feb. 2006.

[16] T. Mahl, A. Hildebrandt, and O. Sawodny, "A Variable Curvature Continuum Kinematics for Kinematic Control of the Bionic Handling Assistant", IEEE Transactions on Robotics, Vol. 30, No. 4, pp. 935-949, 2014.

[17] J.S. Mehling, M.A. Diftler, M. Chu, and M. Valvo, "A Minimally Invasive Tendril Robot for In-Space Inspection", Proceedings BioRobotics 2006 Conference, pp. 690-695, 2006.

[18] Minibuilders. [Online]. Available: http://robots.iaac.net/. [Accessed: 12-Sep-2021].

[19] I. Singh, Y. Amara, A Melingui, P.M. Pathak, and R. Merzouiki, "Modeling of Continuum Manipulators Using Pythagorean Hodograph Curves", Soft Robotics, August 2018.

[20] J. Sustarevas, K. X. Benjamin Tan, D. Gerber, R. Stuart-Smith and V. M. Pawar, "YouWasps: Towards Autonomous Multi-Robot Mobile Deposition for Construction," 2019 IEEE/RSJ International Conference on Intelligent Robots and Systems (IROS), 2019, pp. 2320-2327, doi: 10.1109/IROS40897.2019.8967766.

[21] M. E. Tiryaki, X. Zhang and Q. Pham, "Printing-while-moving: a new paradigm for large-scale robotic 3D Printing," 2019 IEEE/RSJ International Conference on Intelligent Robots and Systems (IROS), 2019, pp. 2286-2291, doi: 10.1109/IROS40897.2019.8967524.

[22] D. Trivedi, C.D. Rahn, W.M. Kier, and I.D. Walker, "Soft Robotics: Biological Inspiration, State of the Art, and Future Research", Applied Bionics and Biomechanics, 5(2), pp. 99-117, 2008.

[23] I. D. Walker, "Continuous Backbone 'Continuum' Robot Manipulators," ISRN Robotics, vol. 2013, p. e726506, Jul. 2013, doi: 10.5402/2013/726506.

[24] R.J. Webster III and B.A. Jones, "Design and Kinematic Modeling of Constant Curvature Continuum Robots: A Review", International Journal of Robotics Research, Vol. 29, No. 13, pp. 1661-1683, November 2010.

[25] M. Wooten and I.D. Walker, "Vine-Inspired Continuum Tendril Robots and Circumnutations", Robotics, 7(3), doi:10.3390/robotics7030058, September 2018., pp. 1-16.